RSC Advances

ROYAL SOCIETY OF CHEMISTRY

www.rsc.org/advances

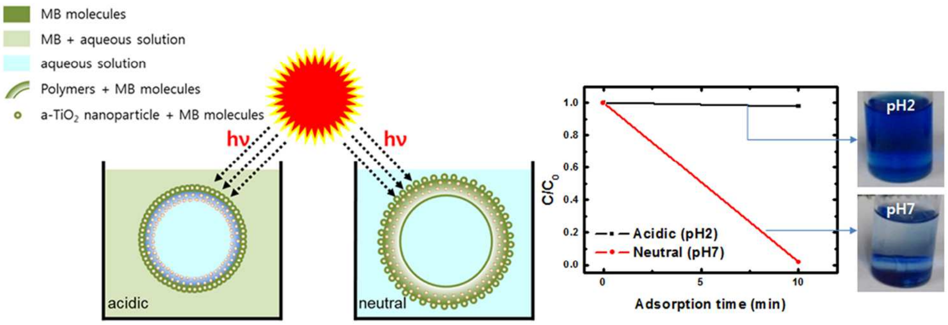

112x44mm (300 x 300 DPI)

Journal Name

ARTICLE

Received 00th January 20xx,
Accepted 00th January 20xx

DOI: 10.1039/x0xx00000x

www.rsc.org/

A facile template-free synthesis of pH-responsive polyelectrolyte/ amorphous TiO_2 composite hollow microcapsules for photocatalysis

Ki-Tae Bang‡[a], Hyung-Seok Lim‡[a], Seong-Jin Park[a] and Kyung-Do Suh*[a]

This paper presents a novel, facile method for fabricating pH-responsive inorganic/organic composite microspheres with hollow structures in the absence of a step for the removal of the core. Using polyelectrolyte (hydrogel) hollow microspheres without a need for further calcination and chemical etching, minimally cross-linked poly(methacrylic acid/ethylene glycol dimethacrylate/3-(trimethoxysilyl) propylmethacrylate), poly(MAA/EGDMA/TMSPM) [pMET] microspheres were prepared by a distillation-precipitation method. Once the pMET microspheres disperse in 2-propanol, the hollow structure is clearly observed and can be maintained more rigidly in a dry state after amorphous TiO_2 (a-TiO_2) is incorporated into the shell of a microsphere by a sol-gel method. The a-TiO_2-incorporated pH-responsive pMET composite [pMET/TiO_2] hollow microspheres were tested as a photocatalyst in acidic and neutral conditions. The photocatalytic performance of the hollow pMET/TiO_2 composite microcapsules under neutral condition was better than that under acidic condition due to their large active surface and strong adsorption ability against methylene blue (MB).

1. Introduction

Titanium dioxide (TiO_2) has received significant attention in the field of photocatalysis because it is non-toxic, recyclable and chemically inert as well as abundant, inexpensive, and has high photocatalytic activity. In particular, nano-sized photoactive materials show better photocatalytic performance due to their large specific surface area. However, they are difficult to separate and recycle from water after use [1-8]. Although some research groups have suggested that activated carbon/photocatalyst composites could be used as carriers to reuse nanoparticles, these composites prevent the irradiation of UV light to TiO_2, and result in lower photocatalytic activity [7,8]. Therefore, UV-transmissible supports for TiO_2 immobilization are needed for effective photocatalytic activity and recycling. Among the promising candidate materials, hydrogels are attractive due to their highly absorbent properties, which are dependent on external environmental conditions [9,10], and light-transparency in aqueous solution. Especially, hollow-structured hydrogels have advantages including fast tunable permeability, high loading efficiency, and easily controlled release based on adjusting the shell thickness and volume of the cavity. Until now, in order to produce hydrogels with a hollow structure, many researchers have suggested synthetic methods, such as template methods including layer-by-layer assembly [11-13] and microfluidics [14,15]. These template methods are complicated and may involve long process time. Previously, our research group reported on hollow hydrogel capsules fabricated by electrostatic attraction between anionic hydrogel networks and cationic cetyl trimethylammonium ion (CTA^+) molecules or Fe^{2+} ions with no need for the removal of the core [16]. The main strategy for this synthesis is the utilization of the phase separation induced by the formation of relatively hydrophobic regions occurring as a consequence of the interaction between negatively-charged hydrogel chains and oppositely-charged surfactants, and consequently generates an internal cavity. We observed that poly(MAA/EGDMA) microspheres have a lower cross-linking density in the core in an acidic aqueous solution due to hydrophobic interaction.

In this paper, we present a facile template-free method of preparing pH-responsive poly(methacrylic acid/ethylene glycol dimethacrylate/3-(trimethoxysilyl) propylmethacrylate), poly(MAA/EGDMA/TMSPM) [pMET] microspheres with a hollow structure without injecting additional molecules like CTA^+, and subsequently hollow pMET microspheres decorated with amorphous TiO_2 (a-TiO_2) nanoparticles using a sol-gel process. The hollow pMET/a-TiO_2 microspheres can capture the cationic organic pollutants in an aqueous solution under alkaline and neutral conditions because the polyelectrolyte body could have a strong negative charge. These composite

---

[a] *Department of Chemical Engineering, College of Engineering, Hanyang University, Seoul, Republic of Korea, 133-791. E-mail: kdsuh@hanyang.ac.kr*
* *Corresponding author (kdsuh@hanyang.ac.kr)*
‡ These authors contributed equally to this work.
Electronic Supplementary Information (ESI) available: [SEM images of poly(MAA/EGDMA) microspheres; OM images of poly(MAA/EGDMA) microspheres dispersed in 2-propanol and water; XRD pattern of pMET/a-TiO_2 composite microcapsules; additional schematic illustration; thermodegradation and photodegradation of MB without photocatalysts; FT-IR spectra of all samples]. See DOI: 10.1039/x0xx00000x

microcapsules exhibit strong dye adsorption ability. The captured organic dyes are decomposed efficiently by photocatalysis of a-TiO_2 nanoparticles embedded in the polyelectrolyte body.

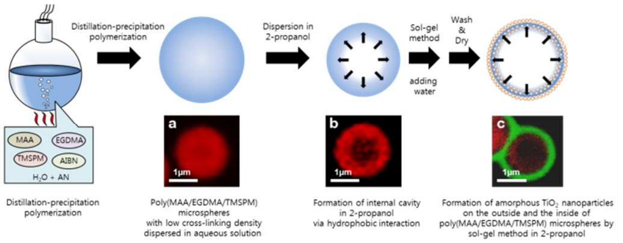

Scheme 1. Schematic illustration for the synthetic process of poly(MAA/ EGDMA/TMSPM)/a-TiO_2 composite microcapsules: CLSM image of the poly(MAA/EGDMA/TMSPM) microspheres dispersed (a) in aqueous solution and (b) 2-propanol, and (c) EDX-maps of (green) titanium and (red) carbon from the hollow poly(MAA/EGDMA/TMSPM)/a-TiO_2 composite microcapsules.

2. Experimental

2. 1 Materials

Methacrylic acid (MAA, 99%, Aldrich), ethylene glycol dimethacrylate (EGDMA, TCI), 3-(trimethoxysilyl) propylmethacrylate (TMSPM, 98%, Aldrich), acetonitrile (AN, Daejung), 2-2’-azoisobutyronitrile (AIBN, Junsei), titanium isopropoxide (97%, Aldrich), iso-propyl alcohol (2-propanol, 99.5%, Yakuri), Rhodamine 123 (Aldrich), and methylene blue (MB, Aldrich) were used as received.

2. 2 Synthesis of Hollow pMET/a-TiO_2 Microcapsules

Monodisperse hollow pMET microspheres were synthesized by distillation precipitation polymerization using EGDMA as a crosslinker. Yang’s group has reported that poly(methacrylic acid-co-3-(methacryloxy)propyltrimethoxysilane) microspheres were synthesized by distillation-precipitation polymerization for preparation of mesoporous silica nanoparticles [17]. In our synthetic process, MAA (3.7 g), EGDMA (0.1 g) and TMSPM (0.2 g) were polymerized at 80 °C for 30 min without mechanical stirring in a medium consisting of AN (68 mL), distilled water (12 mL), and AIBN (0.08 g) as an initiator. After polymerization, residual monomers and the medium were removed by centrifugation with ethanol and 2-propanol. Then, the precipitated particles were dispersed into 2-propanol (200 mL) for 30 min. Titanium isopropoxide (2.5 g) was added into the mixture and stirred for 40 h. The particles were then separated by centrifugation with ethanol. Distilled water (200 mL) was added into the precipitates and continuously stirred for a few hours. The particles were separated by centrifugation and dried in a vacuum at room temperature for one day.

2. 3 Evaluation of Photocatalytic Activity

The hollow pMET/a-TiO_2 composite microcapsules [35 mg poly(MAA/EGDMA/TMSPM)/a-TiO_2] were dispersed into 35 mL of deionized water (DI water). Then, the mixture of 35 mL was added to 90 mL of MB aqueous solution (2.09×10^{-5} M) with different pHs (2, 7 and 11). The above mixture solution was irradiated in a quartz reactor with a circulator to maintain constant temperature and stirred during UV irradiation (300W, 365 nm). Before irradiation, the solution was stirred for 10 min in the dark to reach an adsorption-desorption equilibrium between the photocatalyst and MB. For the experiment under acidic condition, at certain time intervals, 8 mL of the mixture solution was poured into the conical tube each time and centrifuged at 10,000 rpm for 10 min to obtain the clear supernatant. In the case of an experiment under neutral condition, additional processes were demanded. After the neutral supernatant of centrifuged sample was removed, the acidic solution was poured into the conical tube in the same amount as the removed neutral supernatant and then the tube was shaken by hand for 10 min. The sample was centrifuged at 10,000 rpm for 10 min to obtain the clear supernatant. The quantitative determination of MB was performed by measuring its intensity of the absorption band with a UV-vis spectrophotometer. When the existence of MB in composite microcapsules was using FT-IR, the amount of the residual MB dye trapped in the samples under acidic condition is similar to that of samples treated with the acidic aqueous solution after UV irradiation under neutral condition (similar intensities for the absorbance peaks related to the MB molecule, see Figure S8b). In other words, the amount of unreactive MB dye in the swollen samples under neutral condition can be estimated by moving them into the acidic aqueous solution.

2. 4 Characterization

The structural changes and swelling ratio of the composite hollow microcapsules were characterized by optical microscopy (OM), confocal laser scanning microscopy (CLSM), scanning electron microscopy (SEM), focus ion beam (FIB) - SEM, Fourier transform infrared spectroscopy (FT-IR), Raman spectroscopy (Raman), x-ray diffraction analysis (XRD), thermo-gravimetric analysis (TGA), transmission electron microscopy (TEM) and high resolution (HR) - TEM. In the photodegradation efficiency stakes, the progressed sample under the neutral condition was better performance than that under the acidic condition because of different degree of adsorption of MB. It was characterized by a UV-vis spectrophotometer.

3. Results and Discussion

As shown in Scheme 1, in this synthetic process, pMET microspheres with low crosslinking density (less than 5 wt. %) generate a hollow structure in 2-propanol because the hydrophobic interaction of anionic hydrogels becomes stronger. As a result, the hydrophobic parts of the pMET microspheres aggregate with each other, so the dehydration of the hydrogels occurs from the inner to the outer directions to a more stable state, whereas the highly cross-linked (more than 5 wt. %) pMET microspheres contract without generating an internal cavity.

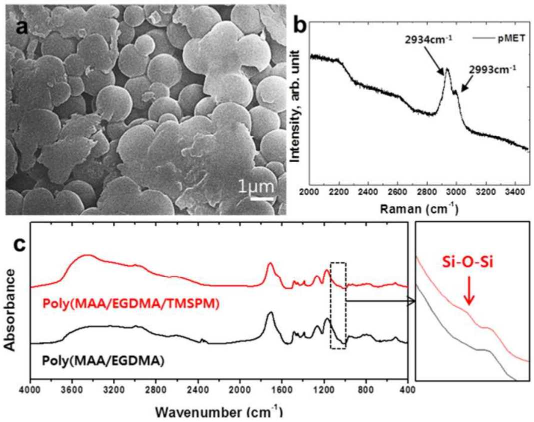

Figure 1. (a) SEM image and (b) Raman spectrum of the pMET microspheres, and (c) FT-IR spectra of the pMET and pME microspheres.

Figure 1a, b and c present the results of SEM and Raman and FT-IR spectroscopy of the pMET microspheres with low crosslinking density. The pMET microspheres exhibited a spherical shape even in the dry state while the poly(MAA/EGDMA) [pME] microspheres in the absence of TMSPM were obtained as a film in the dry state, as shown in Figure S1. Figures 1b and c show Raman spectrum of pMET microspheres and FT-IR spectra of the pME and pMET microspheres. The Raman spectrum shows the characteristic band of the Si-OCH$_3$ group observed at 2934 and 2993 cm^{-1}, implying that the pMET microspheres have some forms of the Si-OCH$_3$ group as a functional site for the proceeding sol-gel reaction [18]. From the FT-IR spectra, the pMET microspheres show the absorption peak corresponding to the Si-O-Si stretching vibration characteristics at 1063 cm^{-1} instead of the Si-OCH$_3$ stretching vibration at 1083 cm^{-1}, while the pME microspheres did not have corresponding peak for either Si-O-Si or Si-OCH$_3$. These results indicated that the pMET microspheres not only have crosslinking networks with Si-O-Si bonding caused by a sol-gel reaction during the polymerization process, but also the Si-OCH$_3$ group. Figure 2 shows CLSM images of the pMET microspheres dispersed in aqueous solution and 2-propanol, respectively. The CLSM image of the pMET microspheres dispersed in aqueous solution exhibits a crosslinking density gradient from the particle center trending outward, as shown in Figure 2a. Since the pMET microspheres have a low crosslinking density and the Si-O-Si bond exhibits secondary crosslinking, a partial hydrophobic interaction may occur. When the particles dispersed in aqueous solution were moved into 2-propanol, the internal cavity was generated from the center of the particle. Figure 2b shows a CLSM image of the hollow-structured pMET microspheres dispersed in 2-propanol. In order to verify the generation of the hollow structure, we carried out an additional experiment. When the dried pMET microspheres were dispersed in water and 2-propanol, the particles dispersed in 2-propanol could not swell, whereas the particles dispersed in water were swollen, as shown in Figure S2. Therefore, the internal cavity was generated by increase in the hydrophobicity of the polymer matrix.

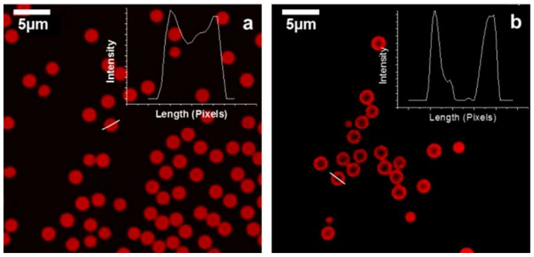

Figure 2. CLSM images of pMET microspheres with low crosslinking density dispersed in (a) aqueous solution and (b) 2-propanol (insets: line profiles) after labeling the carboxyl groups with fluorescent dye (Rhodamine123).

Amorphous TiO$_2$ nanoparticles were incorporated into the hollow pMET microspheres in 2-propanol using titanium isopropoxide. After being stirred for 40 h, the supernatant was removed by centrifugation with ethanol and a large amount of water was added into the reactor with precipitates. The sol-gel reaction occurred in the polymer phase as well as on the surface of the particle. The light-yellow-colored powders were obtained by centrifugation and dried at room temperature. Figure S3 shows XRD patterns of the p(MET) and p(MET)/a-TiO$_2$ composite microspheres and a-TiO$_2$ nanoparticles. XRD pattern of the p(MET)/a-TiO$_2$ composite microspheres exhibited only two broad peaks around 16° and 32° corresponding to the poly(MAA/EGDMA) microspheres. According to the XRD pattern of a-TiO$_2$ nanoparticles that synthesized by sol-gel reaction without polymer templates, TiO$_2$ nanoparticles formed in the polymer phase display low crystallinity, as shown in Figure S3. Figure 3 shows SEM, FIB-SEM, TEM, EDX maps, and HR-TEM images of the hollow pMET/a-TiO$_2$ composite microcapsules. The hollow pMET/a-TiO$_2$ composite microcapsules have a rough surface due to the a-TiO$_2$ nanoparticles coated on the surface of pMET microspheres, as shown in Figure 3a. The focused ion beam (FIB) SEM and TEM images of the hollow pMET/a-TiO$_2$ composite microcapsules indicate that the composite microcapsules have a large internal cavity even in a dry state, as shown in Figures 3b and c.

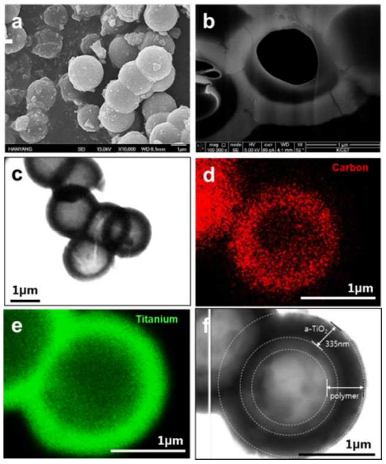

Figure 3. (a) SEM, (b) FIB-SEM, (c) TEM, (d: Carbon, e: Titanium) HR-TEM based EDX maps of the hollow pMET/a-TiO_2 composite microcapsules, and the corresponding (f) HR-TEM image.

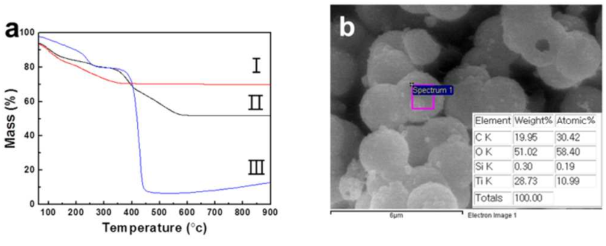

Element	Weight%	Atomic%
C K	19.95	30.42
O K	51.02	58.40
Si K	0.30	0.19
Ti K	28.73	10.99
Totals	100.00	

Figure 4. (a) TGA curves of the [Ⅰ] a-TiO_2 nanoparticles, [Ⅱ] hollow pMET/a-TiO_2 composite microcapsules and [Ⅲ] the pMET microspheres (N_2 atmosphere at 5°C min^{-1}), and (b) SEM image of the hollow pMET/a-TiO_2 composite microcapsules. (Inset: EDX data presents the atomic and weight ratio of the components in the hollow pMET/a-TiO_2 composite microcapsules.)

Figures 3d and e show EDX maps of carbon and titanium elements in the hollow pMET/a-TiO_2 composite microcapsules, and we found that the Ti atoms were diffused into the polymer phase during mechanical stirring in 2-propanol. In addition, the a-TiO_2 nanoparticles were aggregated on the surface of the microcapsules because the residual titanium ions reacted with water outside of the polymer microspheres. We matched the HR-TEM image with EDX maps and drew a domain of a-TiO_2 in the composite hollow microcapsules, as shown in Figure 3f. Figure 4a shows TGA curves of the a-TiO_2 nanoparticles, the hollow pMET/a-TiO_2 and the pMET microspheres. A weight loss of about 30 % was observed during heating to 900 °C in the TGA curve of the a-TiO_2 nanoparticles, as shown in figure 4a (red line). The hollow pMET/a-TiO_2 composite microcapsules exhibited a weight loss in the range of 350~450 °C, attributed to the thermal degradation of the polymer chains (black line), and the residual mass refers to the amount of inorganic materials consisting of SiO_2 and TiO_2 in composite microcapsules at above 450 °C. The TGA curve of the pure pMET microspheres shows the residual mass to be 8.11 % at 450 °C (blue line), which might consist of SiO_2 formed during polymerization. These TGA curves demonstrated that the pMET microspheres have an inorganic segment, and the a-TiO_2 nanoparticles were well incorporated into the hollow pMET/a-TiO_2 microspheres. We also examined the number of elements in composite microcapsules through EDX analysis, as shown in figure 4b. Figure 5a shows OM images of the hollow pMET/a-TiO_2 composite microcapsules dispersed in aqueous solution at different pHs (2, 7 and 11). When the pH value of the aqueous solution containing particles changed from 2 to 11, the particle size increased from 2.1 to 5.3 μm. A plot of the diameter variations of the pMET and hollow pMET/a-TiO_2 composite microcapsules according to pH is shown in Figure 5b. The lower swelling degree of the hollow pMET/a-TiO_2 composite microcapsules is attributed to the amorphous TiO_2 shell coated on the surface of the polymer particle as well as 3D networks of TiO_2 and SiO_2 formed in the polymer phase.

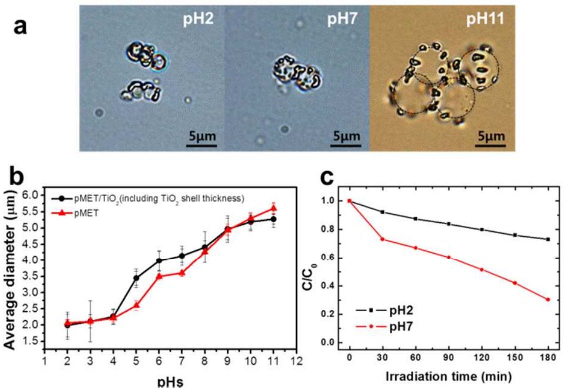

Figure 5. Swelling abilities and photocatalytic activities of the pMET and the hollow pMET/a-TiO_2 composite microcapsules dispersed in aqueous solution with various pHs: (a) OM images of the hollow pMET/a-TiO_2 composite microcapsules dispersed in aqueous solution with three different pHs (pH 2, 7 and 11), (b) the particle size variation of the pMET and the hollow pMET/a-TiO_2 (including a-TiO_2 shell thickness) composite microcapsules dispersed in aqueous solution with various pHs and (c) Photodegradation of methylene blue (MB) of the hollow pMET/a-TiO_2 composite microcapsules under the acidic and neutral conditions.

In the photo-degradation system, the degree of adsorption for organic pollutants on the surface of photocatalysts is very important because the oxidization and reduction of the organic molecules by electron and hole transfers involve interfacial reactions. The concept of photocatalytic degradation in this work is related to two factors; (1) the electrostatic attraction between negative-charged polymer microcapsules and positive-charged organic pollutants and (2) the interfacial area between photocatalysts and organic molecules, as in figure S4. The hollow pMET/a-TiO_2 composite microcapsules are swollen in aqueous solution, as shown above because the hollow polymer chains have negative electrostatic repulsion due to ionization of the carboxylic acid groups. Since methylene blue (MB) has been used as a representative positive-charged dye in aqueous solution, we chose MB to use as an organic pollutant in this experiment.

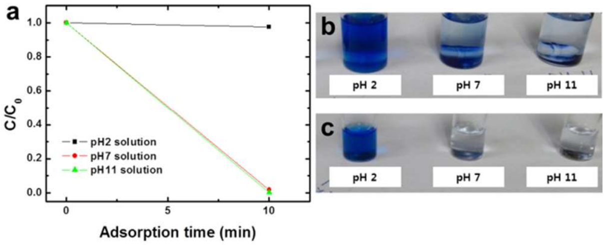

Figure 6. (a) The dye adsorption property of the hollow pMET/a-TiO_2 composite microcapsules for 10 min under different pH conditions and the corresponding digital photographs: (b) MB aqueous solution and particles in vials after centrifugation and (c) supernatant of MB aqueous solution in the absence of particles in vials after centrifugation.

The test of adsorption ability for the hollow pMET/a-TiO_2 composite microcapsules was completed in acidic, neutral and alkali aqueous solutions containing the same concentration of MB. Figure 6a shows that a small amount of MB (about 4%) was adsorbed into pMET/a-TiO_2 microcapsules under acidic condition (pH2), while most MB molecules were adsorbed into pMET/a-TiO_2 microcapsules under neutral (pH7) and alkali (pH11) conditions after magnetic stirring for 10 min. The digital photographs also show that the MB molecules were fully adsorbed in the hollow pMET/a-TiO_2 composite microcapsules under neutral and alkali aqueous solutions, as shown in Figures 6b and c. In order to obtain the exact photocatalytic ability of the hollow pMET/a-TiO_2 microspheres, we regulated three conditions. i) Temperature: the degradation of MB molecules is significantly affected by heat, as shown in Figure S5a. Based on the experimental results, we fixed the temperature in the system to 20 °C.; ii) pH condition: MB concentration in aqueous solution depends on the pH value of the system, as shown in Figure S5b. To minimize the losses of natural degradation for MB, we tested only acidic and neutral conditions.; iii) Stirred during UV irradiation: most photocatalytic experiments were examined with mechanical stirring because the dispersion of photocatalyst powders is important to react with organic pollutants. Our materials are based on the hydrogel having a great affinity with water molecules, which are well floated in aqueous solution without precipitation during mechanical stirring. The photocatalytic ability of the hollow pMET/a-TiO_2 composite microcapsules was evaluated in acidic and neutral aqueous solutions by exposing MB molecules under UV irradiation. The changes in the MB concentration were analyzed as a function of irradiation time, as shown in Figure 5c. The degradation rate of the hollow pMET/a-TiO_2 microcapsules under the neutral condition is much faster than the sample under the acidic condition. Although the TiO_2 nanoparticles incorporated into the hollow polymer microcapsules are amorphous, it is obvious that the MB dye can react with a-TiO_2 under UV irradiation. The photocatalytic efficiency of hollow pMET/a-TiO_2 microcapsules under acidic and neutral conditions can be obtained from figure 5c. After UV irradiation for 180 min, the degradation ratio can reach over 69.74% in the neutral medium, compared with only 26.9% in the acidic medium. Even if the photocatalytic efficiency obtained by subtracting the losses of natural degradation for the hollow pMET/a-TiO_2 microcapsules under the neutral condition was about 35% after UV irradiation for 180 min (Figure S5b), the photocatalytic efficiency under the neutral condition was still higher than that under acidic condition. For acidic condition, a small amount (about 4%, Figure S6a) of MB molecules can be adsorbed on the surface of a-TiO_2 nanoparticles coated on the hydrogel microspheres. However, most MB molecules cannot be diffused into the composite microcapsules because of the reduced negative charge of the composite microcapsules. Therefore, the photocatalytic reaction occurs at the interface between a-TiO_2 nanoparticles coated on the surface of the hollow pMET/a-TiO_2 microcapsules and MB molecules dispersed in the medium. As shown in Figure S6b, on the other hand, in the case of neutral condition, the MB molecules are degraded inside of the swollen microcapsules as well as on their surface because most MB molecules are incorporated into the swollen gels by strong electrostatic attraction between negatively-charged gels and the MB dye together with the adsorption on the surface of a-TiO_2 nanoparticles. Consequently, this better photocatalytic efficiency is attributed to the large surface of reactive materials and the strong adsorption ability of the hollow pMET/a-TiO_2 microcapsules under neutral condition.

Conclusions

In summary, the pH-responsive pMET/a-TiO_2 composite microcapsules with a hollow structure were synthesized by phase separation in the swollen polymer phase with titanium isopropoxide, and then further sol-gel process with the replacement of medium. In our previous studies, the hollow polymeric microcapsules fabricated by electrostatic attraction between negative-charged polymer microspheres and the oppositely-charged surfactants or metal ions without a core-removal process were used as functional drug carriers [18, 19]. Furthermore, the pH-responsive microcapsules were applicable to photocatalytic colloidal system by incorporating a-TiO_2 nanoparticles in the polymer phase. The pMET/a-TiO_2 composite microcapsules exhibited a better photocatalytic performance under neutral condition than that under acidic condition because the typical positive charged organic dye can be absorbed into the ionized pMET phase, and then they are decomposed by a-TiO_2 nanoparticles incorporated throughout the hollow microcapsules under UV irradiation as well as a good dispersion stability. We also confirmed the structural stability of the composite microcapsules under various pH conditions without chipping off a-TiO_2 nanoparticles.

Acknowledgements

This research was supported by Basic Science Research Program through the National Research of Korea (NRF) funded by the Ministry of Education (No. 2014R1A1A2058754).

Notes and references

1 N. M. Mahmoodi, M. Arami, N. Y. Limaee, N. S. Tabrizi, *J. Colloid Interf. Sci.* 2006, **295**, 159.
2 A. Fujishima, T. N. Rao, D. A. Tryk, *J. Photoch. Photobio. C: Photoch. Rev.* 2000, **1** (1), 1.
3 N. Serpone, R. F. Khairutdinov, *Stud. Surf. Sci. Catal.* 1997, **103**, 417.
4 M. R. Hoffmann, S. T. Martin, W. Choi, D. W. Bahnemann, *Chem. Rev.* 1995, **95** (1), 69.
5 M. Addamo, V. Augugliaro, A. D. Paola, E. Garcia-Lopez, V. Loddo, G. Marci, R. Molinari, L. Palmisanoo, M. Schiavello, *J. Phys. Chem. B* 2004, **108**, 3303.
6 H. Choi, E. Stathatos, D. Dionysiou, *Appl. Catal. B* 2006, **63**, 60.
7 X. Wang, Z. Hu, Y. Chen, G. Zhao, Y. Liu, Z. Wen, *Appl. Surf. Sci.* 2009, **255**, 3953.
8 X. Wang, Y. Liu, Z. Hu, Y. Chen, W. Liu, G. Zhao, *J. Hazard. Mater.* 2009, **169**, 1061.
9 A. W. Chan, R. J. Neufeld, *Biomaterials* 2009, **30**, 6119.
10 L. Y. Chu, R. Xie, X. J. Ju, W. Wang, *Smart hydrogel Functional Materials* 2013, **25**.
11 I. Drachuk, O. Shchepelina, M. Lisunova, S. Harbaugh, N.-K. Loughnane, M. Stone, V. V. Tsukruk, *ACS Nano* 2012, **6**, 4266.
12 V. Kozlovskaya, W. Higgins, J. Chen, E. Kharlampieva, *Chem. Commun*. 2011, **47**, 8352.
13 M. Motornov, H. Royter, R. Lupitskyy, Y. Roiter, S. Minko, *Langmuir* 2011, **24**, 15305.
14 T. He, M. Li, J. Zhou, Soft Matter 2012, **8**, 3083.
15 J. Wan, *Polymer* 2012, **4**, 1084.
16 H.-S. Lim, E. Kwon, M. Lee, Y. M. Lee, K.-D. Suh, *Macromol. Rapid Commun.* 2013, **34** (15), 1243.
17 B. Liu, X. Fu, D. Wang, W. Zhang, X. Yang, J. Colloid Interface Sci, 2013, **411**, 98.
18 S. Park, H. Lim, Y. Lee, K. Suh, RSC advances, 2015, **5**, 10081.
19 G. Li, D. Hu, G. Xia, Z. C. Zhang, Top Catal. 2010, **53**, 40.